Efficient Uncertainty Quantification of Stripline Pulse Response using Singular Value Decomposition and Delay Extraction

Andrew Page, Xu Chen
Department of Electrical and Computer Engineering, University of Illinois at Urbana–Champaign, Urbana, IL 61820, USA
ajpage2@illinois.edu, xuchen1@illinois.edu

***Abstract*—This paper demonstrates the use of data post-processing methods with stochastic collocation, an efficient alternative to Monte Carlo sampling, for transient response parametrization in electronic design. This method is applied to find the statistics of the broadband voltage response of a 50Ω terminated stripline with uncertain width, length, and permittivity. Collocation results with post-processing are compared against that of Monte Carlo showing greater accuracy for a low computational budget.**

***Index Terms*—singular value decomposition, delay extraction, stochastic collocation**

I. Introduction

High-speed channel design is an accelerating field that pushes forward the frontier of communications technology. Electromagnetic simulations are employed to predict measures of interest (MoI) for a given channel geometry and material layout, and the parameters defining this layout are chosen to produce results in MoI while obeying various constraints. Upon physical realization of the designed channel, however, parameter uncertainties arise due to manufacturing processes and material properties. These parameter uncertainties can result in significant variability in MoI. A procedure to simulate such variability during the design process would greatly improve the reliability of physical realizations [1], [2]. Monte Carlo sampling (MC) is a method commonly used to address this. This process is reliable but suffers from slow convergence, burdened by the cost of a deterministic simulation, becoming prohibitive for sensitive systems whose simulation is costly.

Stochastic Collocation (SC) is another sampling-based method where the parameter sets are chosen on a sparse subset of the design parameter space, a sparse grid, constructed from tensor products of one-dimensional interpolation grids. MoI are gathered for each parameter set as in MC, but significantly fewer samples are used. The sampled data is then interpolated over the sparse grid to form a surrogate model with which MC is performed, providing more efficient data acquisition.

This paper demonstrates the calculation of broadband voltage response statistics of a stripline with uncertain width W, length L and permittivity ϵ_r. SC is used to efficiently replicate MC-calculated statistics of the voltage response of a Gaussian excitation under such uncertainties [3]. The contribution of this paper is the application of delay extraction (DE) and basis projection via singular value decomposition (SVD) to improve accuracy and efficiency. Section II introduces SC, section III discusses means of improving SC through data processing, section IV discusses numerical results, and concluding remarks are made in section V.

II. Overview of Stochastic Collocation

Maxwell's equations constitute a set of coupled partial differential equations (PDE's) that govern such distributed electrical systems, and many simulation algorithms exist capable of accurately solving them. Due to the parameter uncertainty, modeled by letting each such parameter be represented by a random variable, the governing system is a stochastic PDE with a random solution. SC provides a means of solving such a stochastic PDE by simulating its solution at a set of points in the parameter space, called collocation points or nodes, and creating a surrogate simulation model over the rest of the space. This allows such a stochastic PDE to be approximately solved using deterministic simulations.

The voltage response of a stripline, being a function of its cross-section and material parameters, is a candidate for SC. Such a channel can be described by a three-dimensional parameter vector $\vec{\xi} = [W, L, \epsilon_r]^T$ with voltage output $v(t;\vec{\xi})$. The statistics of $v(t;\vec{\xi})$ can be found with SC by first assembling the set of N collocation points in a $d = 3$ dimensional space, denoted Θ_d^N. This can be done given the ranges of each parameter by first calculating one-dimensional interpolation grids over each parameter and selectively combining these grids into Θ_d^N. Details on this process are given in [4]. Such a grid suffers from the curse of dimensionality, as N trends sharply with dimension d. This is mitigated by controlling the sparsity of the grid with fill level l, trading speed for accuracy.

N full-wave simulations of the response $v(t;\vec{\xi}_j)$ are then run for each point $\vec{\xi}_j \in \Theta_d^N$ where index $j \in \{1, 2...N\}$. The generated data will form an accurate surrogate model when interpolated over the sparse grid, which can be used to efficiently calculate solution statistics. Such data generation has computational cost scaling with the expense of a single simulation. Full wave simulations are often rather expensive, lasting on the order of minutes. Properties of such interpolations can be taken advantage of to accelerate this process. Among such properties is the nesting property, which is satisfied for a SC scheme if for any number of nodes $\beta > \alpha$,

$$\Theta_d^\alpha \subset \Theta_d^\beta. \tag{1}$$

This property allows for cheap grid refinement and is incentive to use rules with such properties.

The MoI considered in this paper is the channel voltage response waveform as a time series vector of length n_t. SC can be applied by treating each time sample as a scalar output and forming individual interpolants for each time step.

III. Data Post-Processing

A. Delay extraction

Time delay is inherent to distributed electrical systems, and is significantly impacted by variations in length and permittivity. Such resulting delay variations cause irregularities in the response waveform from line reflections that make interpolation more difficult via Gibb's phenomenon. A simple delay extraction algorithm is employed to remedy this. For each sampled waveform, the delay time is defined as the first moment the voltage exceeds a preset threshold. Each response is shifted back by its delay, lining up the reception time for each waveform at zero in shifted time. The interpolation is performed over the shifted data, and the extracted delay times are interpolated as well. MC is performed with the surrogate model and waveforms are reconstructed re-introducing the modelled delay into data from the shifted interpolation. This mitigates Gibb's phenomenon in the primary response peak, reducing error in MoI statistics.

B. Singular value decomposition

Creating the surrogate model requires interpolating over Θ_N n_t times, one for each time step. The number of steps n_t is often tens of thousands, as transient reflections pass slowly in low-loss systems. The formation of these numerous interpolations is computationally expensive. A means of mitigating this expense comes in performing a spectral projection on the gathered timeseries data. With this process, the gathered data can be represented as a set of basis coefficients rather than values for n_t time steps. The system response is consistent, mainly characterized by delay and attenuation, implying that the response can be represented in a small timeseries basis. Such a basis expansion can be performed using SVD on the generated data [5]. This process begins with assembling data generated from the sparse grid into matrix $\mathbf{Y} \in \mathbb{R}^{n_t \times N}$ with index $i \in \{1, 2...n_t\}$:

$$Y_{ij} = v(t_i; \vec{\xi}_j). \tag{2}$$

SVD can be performed on this matrix to reveal

$$\mathbf{Y} = \mathbf{U}\mathbf{S}\mathbf{V}^T := \mathbf{U}\mathbf{A} \approx \tilde{\mathbf{U}}\tilde{\mathbf{A}}, \tag{3}$$

where coefficient matrix $\mathbf{A} := \mathbf{S}\mathbf{V}^T \in \mathbb{R}^{n_t \times N}$ and the basis can be read from the columns of $\mathbf{U} \in \mathbb{R}^{n_t \times n_t}$. The rows of $\mathbf{A}$ decrease significantly in magnitude due to the singular nature of $\mathbf{Y}$, implying a reduced basis $\tilde{\mathbf{U}} \in \mathbb{R}^{n_t \times n_{max}}$ with coefficients $\tilde{\mathbf{A}} \in \mathbb{R}^{n_{max} \times N}$ can be formed, where $n_{max} \ll n_t$ can be chosen such that the worst-case approximation error for each waveform in $\mathbf{Y}$, the reconstruction error, is minimized. These basis coefficients can be interpolated over the sparse grid rather than time data for a more cost effective interpolation with controllable error.

IV. Numerical Results

The example studied in this paper is that of a stripline with a 50Ω source and load. The cross-section, depicted in Fig. 1 and summarized in Table I, has five geometric parameters and two material parameters. This example models the uncertain parameters with uniform distributions. The channel is excited with a voltage waveform $v(t)$ and spectrum $V(\omega)$ given by

$$\begin{aligned} v(t) &= \exp\Big\{\frac{-(t-\eta)^2}{2\sigma^2}\Big\} \iff \\ V(\omega) &= \sigma\sqrt{2\pi}\exp\big\{-j\omega\eta\big\}\exp\Big\{-\frac{\sigma^2\omega^2}{2}\Big\} \end{aligned} \tag{4}$$

with pulse width $\eta = \sigma\sqrt{32} = 25$ps. This excitation creates a broadband response while respecting the band-limiting nature of time-domain simulations. An expensive MC will be run to calculate the statistics of this response that will act as a ground truth. Various SC schemes will then be run and compared against MC results of equal sample size to study error convergence. The system will be simulated in a commercial CUDA-enabled FDTD simulator, XFdtd [6], on an Intel® Core™ i7-8700 processor and a NVIDIA GeForce GTX 1080Ti graphics card. Interpolations and sparse grid formation are computed with the MATLAB package TASMANIAN [7], [8].

The collocation schemes used were based on the one-dimensional Clenshaw-Curtis grid [4]. Fill levels of $l = \{5, 7, 9, 11\}$ were used yielding grids of size $N = \{93, 225, 401, 785\}$. Fig. 2 and 3 show the mean and standard deviation of the response calculated by the level $l = 7$ grid alongside DE and SVD post-processing. The raw data clearly struggles to recreate the ground truth MC, burdened by Gibb's phenomena. DE provides a more accurate recreation, mitigating the fluctuations. SVD compression was applied to the DE data showing accurate reconstruction.

Fig. 4 and 5 display the RMS error of each scheme against the ground truth MC. The DE error is lower than its raw counterpart universally. Level 5 and 7 grids, after DE, provide more accurate statistics than an equally expensive MC. Level 9 and 11 grids perform worse due to spurious fluctuations from the DE process. This DE algorithm handles the delay associated with the initial peak well, accurately interpolating the first signal energy to pass. It does not align any subsequent reflections, though the accumulated error is low due to their low amplitudes. More sophisticated DE may be implemented to provide a more suitable interpolation.

SVD compression was performed on each dataset, where n_{max} was chosen such that the maximum RMS reconstruction error never exceeded 1mV, resulting in $n_{max} = \{53, 44, 52, 53\}$ for the four levels. Fig. 4 and 5 show little discrepancy between the DE SVD and DE data, implying that collocation supports such compression. A more accurate compression can be achieved in general by increasing the basis size. Delay extraction improves the SVD projection by increasing regularity in the data, thereby lowering the n_{max} required for a particular error margin. This compression poses benefit in cases where interpolation is expensive, such as if higher bandwidth or finer resolution were desired.

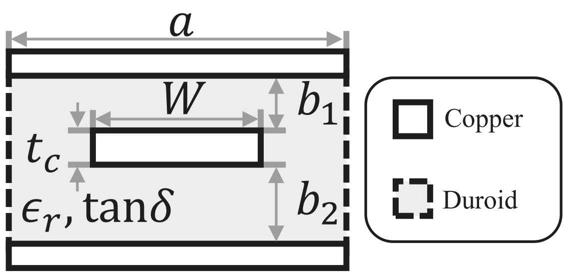

Fig. 1. Stripline cross section diagram and parameter definitions.

TABLE I
PARAMETER VALUES AND DISTRIBUTIONS

Parameter	W(mm)	L(mm)	ϵ_r	a(mm)
Value	$\mathcal{U}(1.0, 1.4)$	$\mathcal{U}(30, 50)$	$\mathcal{U}(2.0, 2.4)$	20
Parameter	b_1(mm)	b_2(mm)	t_c(μm)	$\tan\delta$
Value	0.78	0.78	20	3×10^{-3}

V. Conclusion

This paper has shown that SVD and DE post-processing can accelerate the SC process and provide more accurate quantification of system uncertainty than unprocessed collocation. It was shown that SC supports SVD-based data compression. A simple DE algorithm was introduced and provided more accurate response statistics over a variety of grid sizes. Further work on delay extraction may allow high level grids to outpace MC and is under investigation.

Acknowledgment

This material is based upon work supported by the National Science Foundation under Grant No. CNS 16-24811 - Center for Advanced Electronics through Machine Learning (CAEML) and its industry members.

References

[1] D.-H. Huang, A. C. Cangellaris, and X. Chen, "Stochastic-Galerkin Finite-Difference Time-Domain for Waves in Random Layered Media," in *2020 IEEE MTT-S International Conference on Numerical Electromagnetic and Multiphysics Modeling and Optimization (NEMO)*. Hangzhou, China: IEEE, Dec. 2020, pp. 1–4.

[2] D. Xiu and J. S. Hesthaven, "High-order collocation methods for differential equations with random inputs," *SIAM Journal on Scientific Computing*, vol. 27, no. 3, pp. 1118–1139, 2005. [Online]. Available: https://doi.org/10.1137/040615201

[3] A. Deutsch, R. S. Krabbenhoft, K. L. Melde, C. W. Surovic, G. A. Katopis, G. V. Kopcsay, Z. Zhou, Z. Chen, Y. H. Kwark, T.-M. Winkel, X. Gu, and T. E. Standaert, "Application of the short-pulse propagation technique for broadband characterization of pcb and other interconnect technologies," *IEEE Transactions on Electromagnetic Compatibility*, vol. 52, no. 2, pp. 266–287, 2010.

[4] D. Xiu, *Numerical Methods for Stochastic Computations: A Spectral Method Approach*. Princeton University Press, Jul. 2010.

[5] P. Manfredi and R. Trinchero, "A Data Compression Strategy for the Efficient Uncertainty Quantification of Time-Domain Circuit Responses," *IEEE Access*, vol. 8, pp. 92 019–92 027, 2020.

[6] Remcom, "Xfdtd," 2021.

[7] M. Stoyanov, D. Lebrun-Grandie, J. Burkardt, and D. Munster, "Tasmanian," 9 2013. [Online]. Available: https://github.com/ORNL/Tasmanian

[8] M. Stoyanov, "User manual: Tasmanian sparse grids," Oak Ridge National Laboratory, One Bethel Valley Road, Oak Ridge, TN, Tech. Rep. ORNL/TM-2015/596, 2015.

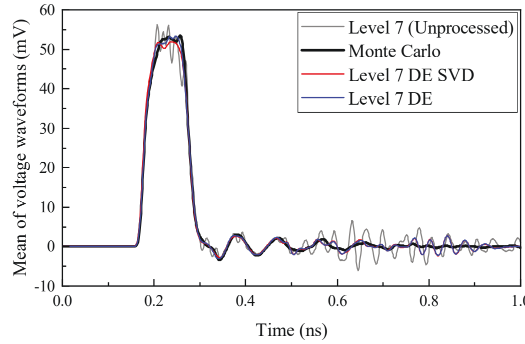

Fig. 2. Calculated mean of the response voltage time series with various methods.

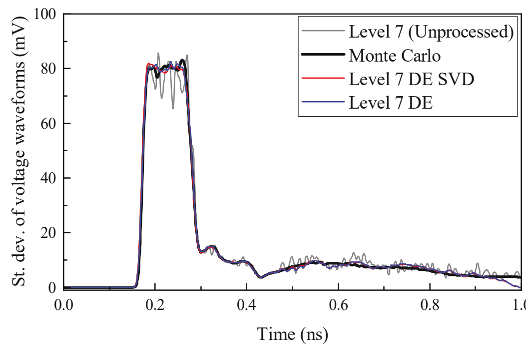

Fig. 3. Calculated standard deviation of the response voltage time series with various methods.

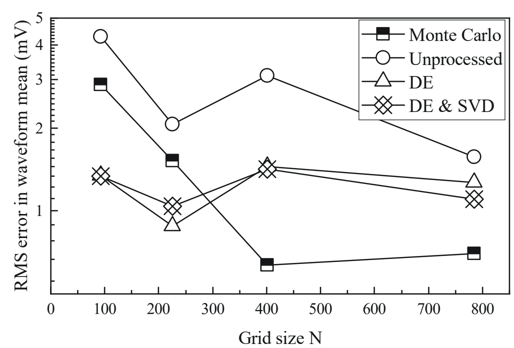

Fig. 4. Comparison of error in mean against ground truth MC.

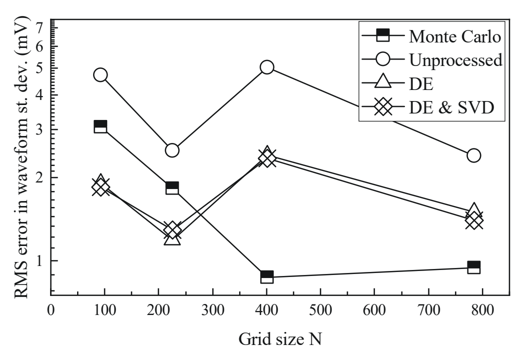

Fig. 5. Comparison of error in standard deviation against ground truth MC.